



ChemComm

Conformational control via sequence for a heteropeptoid in water: coupled NMR and Rosetta modelling

| | |
|---------------|--------------------------|
| Journal: | <i>ChemComm</i> |
| Manuscript ID | CC-COM-04-2021-001992.R3 |
| Article Type: | Communication |
| | |

SCHOLARONE™
Manuscripts

COMMUNICATION

6 Conformational control via sequence for a heteropeptoid in 7 water: coupled NMR and Rosetta modelling

8 Trideep Rajale,^{‡a} Jacob C. Miner,^{‡b,c} Ryszard Michalczyk,^c M. Lisa Phipps, Jurgen G. Schmidt,^c
9 Robert D. Gilbertson,^d Robert F. Williams,^c Charlie E. M. Strauss,^{*c} and Jennifer S. Martinez^{*e,f}

1 Received 00th July 20xx,
2 Accepted 00th July 20xx

3 DOI: 10.1039/x0xx00000x

10 **We report a critical advance in the generation and characterization
11 of peptoid hetero-oligomers. A library of sub-monomers with
12 amine and carboxylate side-chains are combined in different
13 sequences using microwave-assisted synthesis. Their sequence-
14 structure propensity is confirmed by circular dichroism, and
15 conformer subtypes are enumerated by NMR. Biasing the ψ -angle
16 backbone to *trans* (180°) in Monte Carlo modelling
17 favors *i* to *i*+3 naphthyl-naphthyl stacking, and matches
18 experimental ensemble distributions. Taken together, high-yield
19 synthesis of heterooligomers and NMR with structure prediction
20 enables rapid determination of sequences that induce secondary
21 structural propensities for predictive design of hydrophobic
22 peptidomimetic foldamers and their future libraries.**

23 Peptoids are peptidomimetic oligomers composed of *N*-substituted
24 glycine units with potential applications in fields spanning
25 biomedical to the materials sciences, provided their macromolecular
26 structures can be controlled.^{1–8} Peptoids have the same C–N
27 backbone repeat as naturally-occurring proteins, but the
28 substitution makes the backbone achiral and precludes any (protein-
29 like) backbone hydrogen-bonding networks (Fig. 1).^{9,10} Chirality
30 backbone hydrogen-bonding are responsible for energetically
31 preferred local structural biases in proteins and are key elements
32 of ‘secondary structure’. These protein secondary structures,
33 combination with side-chain interactions and chemical functions
34 (i.e. hydrophobicity, polarity, π -stacking, and hydrogen bonds),

dictate three-dimensional folding and function. Thus, the challenge
for peptoid-based foldamers, is developing control over structure
and design at the level of proteins. This challenge requires
identification of sequence-to-structure relationships, while
developing comprehensive methods to generate, *individual, self-
folding, water-soluble* hetero-peptoids.^{11–13} The first step toward this
goal is to design and model peptoids with the chemical and structural
functionality of protein secondary structures.

Encouragingly, several publications suggest individual peptoids can
achieve three-dimensional order. Wu et. al. and Patch et. al.
demonstrated that hydrophobic peptoid homooligomers, could
assume secondary structure in organic solvents or when embedded
into lipid membranes.^{14,15} Armand et. al. demonstrated that three-
dimensional order can be achieved for a hetero-oligomeric pentamer
in methanol.¹⁶ Finally, Darapaneni et. al. partially improved upon
hydrophobic peptoid solubility by post-synthetic addition of
piperazines to a homooligomer, demonstrating that the peptoid
maintained its secondary structure once transferred into aqueous
phase.¹⁷ Most of these studies used bulky chiral side-chains to reduce
peptoid conformational freedom, providing an approach to generate
secondary structural elements.^{14–18} Unfortunately, these peptoids
lack the structural and sidechain chemical precision of proteins, or
their hydrophilicity, precluding downstream complex functions such
as catalysis and molecular recognition in any peptoid foldamer.
Further, many of these studies only rely on circular dichroism (CD) to

* Corresponding authors.

^a Center for Integrated Nanotechnologies, (CINT), Los Alamos National Laboratory,
Los Alamos, NM 87545, United States.

^b Theoretical Biology and Biophysics, Los Alamos National Laboratory, Los Alamos,
NM 87545, United States.

^c Bioscience Division, Los Alamos National Laboratory, Los Alamos, NM 87545,
United States.

^d Materials Science and Technology Division, Los Alamos National Laboratory, Los
Alamos, NM 87545, United States.

^e Center for Materials Interfaces in Research and Applications, Northern Arizona
University, Flagstaff, Arizona 86011, United States.

^f Department of Applied Physics and Materials Science, Northern Arizona
University, Flagstaff, Arizona 86011, United States.

^g † Electronic Supplementary Information (ESI) available: [details of any
supplementary information available should be included here]. See
DOI: 10.1039/x0xx00000x

^a Center for Integrated Nanotechnologies, (CINT), Los Alamos National Laboratory,
Los Alamos, NM 87545, United States.

^b Theoretical Biology and Biophysics, Los Alamos National Laboratory, Los Alamos,
NM 87545, United States.

^c Bioscience Division, Los Alamos National Laboratory, Los Alamos, NM 87545,
United States.

^d Materials Science and Technology Division, Los Alamos National Laboratory, Los
Alamos, NM 87545, United States.

^e Center for Materials Interfaces in Research and Applications, Northern Arizona
University, Flagstaff, Arizona 86011, United States.

^f Department of Applied Physics and Materials Science, Northern Arizona
University, Flagstaff, Arizona 86011, United States.

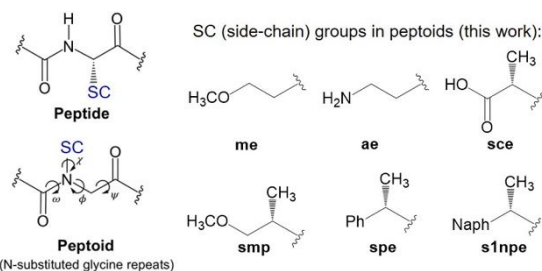
* corresponding authors

‡ These two authors contributed equally to this work

† Electronic Supplementary Information (ESI) available: [details of any supplementary
information available should be included here]. See DOI: 10.1039/x0xx00000x

1 characterize structures.¹⁸⁻²³ Finally, beyond the limited structural
 2 understanding achievable from ensemble measurements (e.g. CD),
 3 cannot resolve ensemble heterogeneity as well as NMR), past
 4 modelling of peptoid structures have assumed that peptoid
 5 backbones had a flexibility similar to peptide backbones: limiting the
 6 potential for studying the driving forces for peptoid secondary
 7 structure formation.

8 These facts open many opportunities for greatly improving aqueous
 9 peptoid design by merging the insights obtained from previous
 10 analyses of peptoids²⁴⁻²⁷ and leveraging refined synthetic protocols
 11 with characterization by nuclear magnetic resonance spectroscopy
 12 (NMR)¹⁷ and molecular modelling.²⁸⁻³⁴



13 **Fig. 1.** Structural comparison of peptide and peptoid backbones
 14 (backbone dihedral angles ω , ϕ , ψ , and side-chain angle χ shown). SC
 15 represents the side-chain group.

17 In this study we demonstrate an integrated methodology for
 18 developing short hetero-oligomers of individual, water-soluble
 19 peptoids, with conformational biases based on sequence. Our aim is
 20 to identify patterns that limit the secondary structure palette
 21 sufficiently to allow folding to occur, and to measure the degree of
 22 diversity – conformational freedom – in induced secondary
 23 structures. Using a microwave synthesis method that facilitates
 24 efficient hetero-peptoid synthesis, and incorporates polar,
 25 hydrophilic side-chains with amine and carboxyl functional groups,
 26 we achieved high-purity syntheses. We refined the ensemble
 27 characterization of CD by incorporation of NMR to determine the
 28 diversity of structures in solution. Finally, we employed a modelling
 29 technique with demonstrated success for peptides, and extensible
 30 methods for peptoids³⁴⁻³⁶, and for the first time demonstrated the
 31 importance of enforcing peptoid-specific backbone parameters (i.e.
 32 $\psi \sim 180^\circ$).^{28,29} The success of this approach is highlighted for a
 33 pentameric peptoid sequence that exhibits a restricted set of
 34 conformers in aqueous solution.

35 The submonomer solid-phase synthesis developed by Zuckermann is
 36 ubiquitous for synthesis of up to 50-mer peptoids (Supporting
 37 Information, Scheme S1, ESI[†]).^{37,38} However, long reaction times
 38 (>2.5 hrs per residue), high reagent stoichiometry requirements, and
 39 lack of commercial precursors for many side-chains limit the
 40 potential for high-throughput combinatorial production of
 41 peptoids.³⁹

42 Microwave irradiation can accelerate solid-phase synthesis of
 43 peptoids; however, previous applications focused exclusively on
 44 homo-oligomeric non-water soluble peptoids and used excess
 45 submonomer precursors.^{40,41} Here we expand this technique to the
 46 domain of water-soluble peptoid heteropolymers, enabling an

economical synthetic method that is amenable to diverse
 submonomer precursors.

The various submonomers used to construct our peptoid hetero-
 oligomer library are shown in Fig. 1. Critically, these side-chains
 supply hydrophobicity, hydrophilicity, chirality, and hydrogen
 bonding otherwise absent from peptoid backbones. Further, we
 incorporated chiral phenyl (Nspe) or chiral naphthyl (Ns1npe)
 submonomers periodically at *i* and *i*+3 positions in order to favor π -
 π stacking, which we anticipated could induce polyproline type-I-like
 turns.^{42,43}

To compare the performance of microwave-assisted synthesis to the
 conventional batch submonomer method, we first synthesized an α -
 chiral pentameric peptoid with naphthyl (Ns1npe) groups (**H5** in
 Table 1).¹⁴ We found that conventional synthesis of **H5** at room
 temperature required approximately 21 hrs for coupling five peptoid
 submonomers. This reaction required high stoichiometric
 equivalents of bromoacetic acid, N,N'-diisopropylcarbodiimide (DIC)
 and submonomers to produce crude **H5** at 66% purity. Under
 optimized microwave conditions the reaction time was reduced to
 approximately 2.5 hrs, required fewer equivalents of submonomers,
 and produced crude **H5** at 90% purity (Supporting Information Fig.
 S1, ESI[†]). Additional purification to >95% homogeneity was achieved
 via semi-preparative reverse-phase HPLC (Fig. S2, for details see
 ESI[†]), and these samples were used in our structural analyses.

While purity in any one synthesis can be achieved by post-synthetic
 purification, the crude purity of our techniques will be a critical
 feature of future, high-throughput combinatorial applications and
 peptoid design.

Table 1. Microwave synthesis of peptoid hetero-oligomers

| entry | peptoid sequence ^a | MS ^b | purity (%) ^c |
|-----------|--|-----------------|-------------------------|
| H1 | H-Nspe-Nsce-Nme-Nspe-Nsce-NH ₂ | 713.5 | 94 |
| H2 | H-Nspe-Nae-Nme-Nspe-Nae-NH ₂ | 655.4 | 91 |
| H3 | H-Nae-Nspe-Nae-Nme-Nspe-NH ₂ | 669.8 | 90 |
| H4 | H-Ns1npe-Nae-Nme-Ns1npe-Nae-NH ₂ | 754.9 | 87 |
| H5 | H-Ns1npe-Nae-Nae-Ns1npe-Nsce-NH ₂ | 768.9 | 90 |
| H6 | H-Nae-Nspe-Nme-Nae-Nspe-NH ₂ | 654.8 | 84 |
| H7 | H-Nspe-Nae-Nsmp-Nspe-Nae-NH ₂ | 668.8 | 87 |

^a Peptoids were synthesized on Rink amide resin (0.05 mmol scale). Nae submonomer as Boc-protected and Nsce submonomer as *tert*-butyl protected. ^bESI-MS data. ^cPercent purity estimated by analytical reversed-phase HPLC of crude dry peptoid after ether precipitation and washing.

To demonstrate sequence effects on the structure of peptoids, a
 small library of hetero-oligomers, with an expanded repertoire of
 chemical functionality, was prepared by our microwave protocol on
 a solid support (Table 1). Collectively, good to excellent (84-94%)
 crude purity was obtained in short (5-hr) reactions for all sequences
 in Table 1. Moreover, we were able to synthesize octamer hetero-
 oligomers (**H8** and **H9**) with moderate (62-68%) purities (Table S1).

Secondary structure preference was first assessed using CD. Each
 peptoid showed distinct CD patterns, varying in peak wavelength and
 intensity (degree of ellipticity), suggesting the CD pattern depends
 on the sequence (Fig. S3, ESI[†]). In contrast to phenyl-containing
 peptoids (**H1**, **H2**, **H3**, **H6** and **H7**, Supporting Information Fig. S3A,

ESI[†]), the naphthyl-containing peptoids (**H4** and **H5**, Supporting Information Fig. S3B, ESI[†]) show strong features at 230 nm and 245 nm, suggesting a chiral preference induced in the backbone structure. While **H4** and **H5** have the same number of naphthyl groups, the **H4** peaks are larger and sharper, suggesting a more stable structure than **H5** (Fig. S3B, ESI[†]), as also observed in NMR. Subsequent analyses therefore focus strictly on structures of **H4**.

Assignments by Fuller *et al.* suggests that minima near 230 nm are analogous to helix bands in peptides, and represent *i* to *i*+3 interactions consistent with naphthyl-naphthyl stacking.⁴⁴ However, the lack of defined aqueous solution phase structures of hetero-peptoids limits the interpretation of CD for these compounds and only describes their average helicity.¹⁶

We employed NMR to determine the occupancies of distinguishable conformational motifs. This contrasts with how NMR is normally employed, where peaks are assigned, coupling provides contact information, and through-space coupling provides distance information leading to determination of a structure. However, in complex mixtures it is nearly always the case that NMR peaks can be observed but not assigned. Even so, critical information can often be found in the spectra. When conformational motifs comprise the majority of signal, we can partition these into states and determine an occupancy ratio. Thus, we can estimate the occupancy of certain conformers even though we can neither determine structures nor assuredly associate NMR peaks with particular defined states.

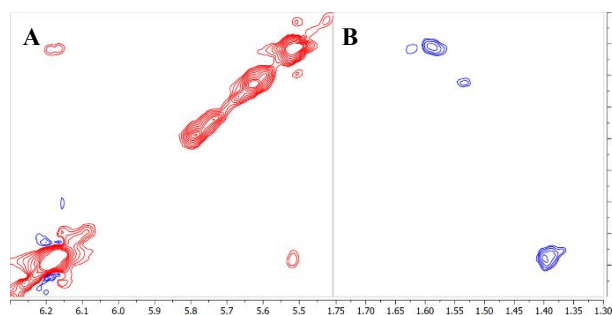


Fig. 2. Structural analysis of **H4** using ROESY spectra (400 ms mixing time) shows two major conformers. **(A)** Exchange cross-peaks at 5.5 ppm and 6.2 ppm indicate two long-lived, exchanging conformers. **(B)** Through-space magnetization shows both conformers exist simultaneously based on opposite-sign cross-peaks (blue).

The observability of any cross-peak in the TOCSY or ROESY spectra (Fig. 2 and Figs. S4-S6) necessarily indicates a conformational state that is well occupied on NMR time scale. Although we cannot assign these peaks, we can simply count the largest peaks and put a lower-bound on the minimum fraction of the total population in these. From spectral deconvolution of 1D spectra for **H4** peptoid we obtained approximately 24 doublets, which would correspond to 22 different conformational states; most of them present in very small quantities (see ESI[†]). Crucially, the ROESY intensity of the two main conformers comprises 80% of the total intensity observed, and deconvolved 1D NMR intensity fraction is roughly 65%. This difference is consistent with the small fractions represented by several of the conformers (as deduced from 1D deconvolution) not being observed in the ROESY spectra with lower signal to noise.

ratio between the two main conformers by 1D NMR is approximately 2:1 (see SI). Further, the existence of exchange peaks for the major conformers indicate two long-lived peptoid conformers that interconvert. However, not every exchange peak is observable due to a combination of factors: 1) The exchange rates are outside of the range of the experimental modality, 2) overlapping spectra, 3) signals too close to the diagonal, or 4) signal is below the noise threshold.

An important bridge toward predictive design depends on closing the gap between models and experiments. Using Rosetta,^{34,45} an efficient biomolecular structural sampling tool with MC capabilities and peptoid parameters,⁴⁵⁻⁴⁷ we generated ensembles of the **H4** peptoid that involve initializing the ψ angle to 180°. Comparisons with NMR ensembles of **H4** peptoid confirms the anticipated *i* to *i*+3 secondary structure with a stacking metric based on pairwise distances of six-membered rings.⁴⁸ Distances between proximal and distal rings in naphthyl side-chains (Fig. S16, ESI[†]), and the average of both values in each conformer (Fig. 3) describes two general conformer types: 'stacked' (3–6 Å), and 'unstacked' (6–10 Å), with all other conformers described by several minor peaks at naphthyl-naphthyl distances >10.0 Å. These two conformers account for 86% of the ensemble (27% stacked, 59% unstacked) and demonstrate that the accessible basins of attraction for the energy landscape are dominated by two conformers. The major finding here is that when ψ is initialized to 180°, Rosetta, like NMR, identifies two major conformers rather than a continuum of states (our precision is not sufficient to say if the larger Rosetta population corresponds to the more populated conformer in NMR).

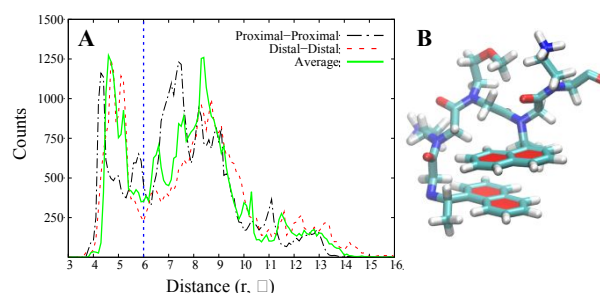


Fig. 3. **(A)** Naphthyl-naphthyl distances in peptoid **H4** divides the ensemble into preferred conformers consistent with NMR and CD results. Distances between naphthyl ring centers show well-defined peaks corresponding to 'stacked' (3 < r ≤ 6 Å) and 'unstacked/extended' (6 < r ≤ 10 Å) conformers (separated by a dashed blue line). **(B)** The median centroid structure for the lowest energy conformers in the **H4** ensemble.

While it has long been assumed that π - π stacking of *i* to *i*+3 species was the critical component for reducing peptoid conformational flexibility, our results instead suggest that the reduced flexibility of the ψ backbone angle may be the determining factor for limiting peptoid conformational freedom (Fig. S17 & S19, ESI[†]).

In conclusion, this work represents a crucial step toward design of peptoid secondary structural elements, and their larger foldamers, with the chemical diversity required to mimic the complex functions of proteins (e.g. catalysis and molecular recognition). In addition to developing a rapid, economical synthetic procedure to generate

1 high-purity peptoid hetero-oligomers (required for downstream
 2 combinatorial production of peptoid foldamers from suites of unique
 3 secondary structural elements), we confirm through CD and NMR
 4 experiments, and molecular modelling, the significance of sequence
 5 on structural propensity. Based on CD and NMR spectroscopy
 6 interpretations, we observe a significant dependence of structural
 7 propensity on sequence. Detailed NMR analysis of the naphthyl-
 8 containing **H4** hetero-oligomeric peptoid indicates the ensemble
 9 dominated by two major conformers, and Monte Carlo modeling
 10 recapitulates these results with the critical inclusion of a peptoid
 11 specific bias (ψ backbone angle initialization at 180°) (Fig. S17 & S19,
 12 ESI†). Model conformers of the **H4** peptoid ensemble can be
 13 represented by (1) a close naphthyl-naphthyl stacking arrangement,
 14 and (2) more extended conformations. Thus, incorporating peptoid-
 15 specific backbone parameters with naphthyl-naphthyl stacking is a
 16 successful and re-usable design principle for inducing constrained
 17 secondary structure in *individual, self-folding, water-soluble* hetero-
 18 oligomeric peptoids: a critical step towards synthesis of three-
 19 dimensional foldamers that mimic the natural chemical diversity
 20 found in nature.

21 This study was partially supported by the Laboratory-Directed
 22 Research and Development program of Los Alamos National
 23 Laboratory (20160044DR) and the State of Arizona Technology
 24 Research Initiative Fund (TRIF), administered by the Arizona Board
 25 Regents, through Northern Arizona University (J.S.M.). This work
 26 was performed, in part, at the Center for Integrated
 27 Nanotechnologies, an Office of Science User Facility operated for the
 28 U.S. Department of Energy (DOE). Los Alamos National Laboratory is
 29 operated by Triad National Security, LLC, for the National Nuclear
 30 Security Administration of the U.S. Department of Energy under
 31 contract No. 89233218CNA000001

32 Conflicts of interest

33 There are no conflicts of interest to declare.

- 34
 35 1 R. J. Simon, R. S. Kania, R. N. Zuckermann, V. D. Huebner,
 36 A. Jewell, S. Banville, S. Ng, L. Wang, S. Rosenberg, C. K.
 37 Marlowe, *PNAS*, 1992, **89**, 9367.
 38 2 N. Gangloff, J. Ulbricht, T. Lorson, H. Schlaad, R. Luxenhofer,
 39 *Chem. Rev.* 2016, **116**, 1753.
 40 3 K. Kirshenbaum, A. E. Barron, R. A. Goldsmith, P. Armand,
 41 E.K. Bradley, K. T. V. Truong, K. A. Dill, F. E. Cohen, R. N.
 42 Zuckermann, *PNAS*. 1998, **95**, 4303.
 43 4 M.L Huang, D. Ehre, Q. Jiang, C. Hu, K. Kirshenbaum, M. P.
 44 Ward, *PNAS*. 2012, **109**, 19922.
 45 5 D. J. Murray, J. H. Kim, E. M. Grzincic, S. C. Kim, A. R. Abate,
 46 R. N. Zuckermann, *Langmuir*. 2019, **35**, 13671.
 47 6 R. Gopalakrishnan, A. I. Frolov, L. Knerr, W. J. Drury, E.
 48 Valeur, *J. Med. Chem.* 2016, **59**, 9599.
 49 7 L. M. S. Wolf, S. L. Servos, M. A. Moss, *J. Neurol. Neurosurg.*
 50 *2017*, **2**, 1.
 51 8 J. Morimoto, et. al. *J. Am. Chem. Soc.* 2020, **142**, 2277
 52 9 J. Sun, R. N. Zuckermann, *ACS Nano*. 2013, **7**, 4715.
 53 10 R. N. Zuckermann, *J. Pept. Sci.* 2011, **96**, 545.

- 11 K. Huang, C.W. Wu, T. J. Sanborn, J. A. Patch, K.
 Kirshenbaum, R. N. Zuckermann, A. E. Barron, I.
 Radhakrishnan, *J. Am. Chem. Soc.* 2006, **128**, 1733.
 12 T. S. Burkoth, E. Beausoleil, S. Kaur, D. Tang, F. E. Cohen, R.
 N. Zuckermann, *Chem. Biol.* 2002, **9**, 647.
 13 A. W. Wijaya, A. I. Nguyen, L. T. Roe, G. L. Butterfoss, R. K.
 Spencer, N. K. Li, R. N. Zuckermann, *J. Am. Chem. Soc.* 2019,
141, 19436.
 14 C. W. Wu, T. J. Sanborn, K. Huang, R. N. Zuckermann, A. E.
 Barron, *J. Am. Chem. Soc.* 2001, **123**, 6778.
 15 J. A. Patch, A. E. Barron. *J. Am. Chem. Soc.* 2003, **125**, 12092.
 16 P. Armand, K. Kirshenbaum, R. A. Goldsmith, S. Farr-Jones, A.
 E. Barron, K. T. V. Truong, K. A. Dill, D. F. Mierke, F. E. Cohen,
 R. N. Zuckermann, E. K. Bradley, *PNAS*. 1998, **95**, 4309.
 17 C. M. Darapaneni, P. J. Kaniraj, G. Maayan. *Org. Biomol.*
Chem. 2018, **16**, 1480.
 18 T. J. Sanborn, C. W. Wu, R. N. Zuckermann, A. E. Barron,
Biopolymers. 2002, **63**, 12.
 19 B. C. Gorske, B. L. Bastian, G. D. Geske, H. E. Blackwell, *J. Am.*
Chem. Soc. 2007, **129**, 8928.
 20 S. Hoyas, E. Halin, V. Lemaury, J. De Winter, P. Gerbaux, J.
 Cornil, *Biomacromolecules*. 2020, **21**, 903.
 21 D. Gimenez, J.A. Aguilar, E. H. C. Bromley, S. L. Cobb, *Angew.*
Chem. Int. Ed. 2018, **57**, 10549.
 22 D. Gimenez, G. Zhou, M. F. D. Hurley, J. A. Aguilar, V. A.
 Voelz, S. L. Cobb, *J. Am. Chem. Soc.* 2019, **141**, 3430.
 23 R. Armand, K. Kirshenbaum, A. Falicov, R.L. Dunbrack, K. A.
 Dill, R. N. Zuckermann, F. E.; Cohen, *Fold. Des.* 1997, **2**, 369.
 24 C. W. Wu, K. Kirshenbaum, T. J. Sanborn, J. A. Patch, K.
 Huang, K. A. Dill, R. N. Zuckermann, A. E. Barron, *J. Am.*
Chem. Soc. 2003, **125**, 13525.
 25 G. Angelici, N. Bhattacharjee, O. Roy, S. Faure, C. Didierjean,
 L. Jouffret, F. Jolibois, L. Perrin, LC; Tallefumier, *Chem.*
Commun. 2016, **52**, 4573.
 26 O. Roy, G. Dumonteil, S. Faure, L. Jouffret, A. Kriznik, C.
 Taillefumier, *J. Am. Chem. Soc.* 2017, **139**, 13533.
 27 M. Rzeigui, M. Traikia, L. Jouffret, A. Kriznik, J. Khiari, O. Roy,
 C. Taillefumier, *J. Org. Chem.* 2020, **85**, 2190.
 28 V. A. Voelz, K. A. Dill, I. Chorny. *Biopolymers*. 2011, **96**, 639.
 29 G. L. Butterfoss, P. D. Renfrew, B. Kuhlman, K. Kirshenbaum,
 R. Bonneau. *J. Am. Chem. Soc.* 2009, **131**, 16798.
 30 J. Laursen,; P. Harris; P. Fristrup, C. A. Olsen. *Nat. Commun.*
 2015, **6**, 7013.
 31 J. A. Schneider, T.W. Craven, A.C. Kasper, et. al. *Nat. Comm.*
 2018, **9**, 4396.
 32 Roe, L.T., et. al. *Biopolymers*. 2019, **110**, e23267
 33 G. J. Rocklin, T. M. Chidyausiku, I. Goresnik, et. al. *Science*.
 2017, **357**, 168.
 34 C. A. Rohl, C. E. M. Strauss, K. M. S. Misura, D. Baker,
Methods in Enzymology, Academic Press, 2004.
 35 R. K. Jha, T. Gaiotto, A. R. M. Bradbury, C. E. M. Strauss,
Protein Eng. Des. Sel. 2014, **27**, 127.
 36 R. K. Jha, S. Chakraborti, T. L. Kern, D. L. Fox, C. E. M. Strauss,
Proteins. 2015, **83**, 1327.
 37 R. N. Zuckermann, J. M. Kerr, S. B. H. Kent, W. H. Moos, *J.*
Am. Chem. Soc. 1992, **114**, 10646.
 38 G. M. Figliozzi, R. Goldsmith, S. C. Ng, S. C. Banville, R. N.
 Zuckermann, *Methods in Enzymology*, Academic Press, 1996.
 39 C. O. Kappe, *Angew. Chem. Int. Ed.* 2004, **4**, 6250.
 40 H. J. Olivos, P. G. Alluri, M. M. Reddy, D. Salony, T. Kodadek,
Org. Lett. 2002, **4**, 4057.
 41 B. C. Gorske, S. A. Jewell, E. J.; Guerard, H. E. Blackwell, *Org.*
Lett. 2005, **7**, 1521.
 42 Shin, H.-M.; Kang, C.-M.; Yoon, M.-H.; Seo, J. *Chem.*
Commun. 2014, **50**, 4465.
 43 Stringer, J. R.; Crapster, J. A.; Guzei, I. A.; Blackwell, H. E. *J.*
Am. Chem. Soc. 2011, **133**, 15559.

Journal Name

COMMUNICATION

- 1 44 Fuller, A. A.; Yurash, B. A.; Schaumann, E. N.; Seidl, F. *J. Org.*
2 *Lett.* 2013, **15**, 5118.
- 3 45 Leaver-Fay, A.; et. al. *Methods in Enzymology*, Johnson, M.
4 L.; Brand, L., Eds. Academic Press: 2011; Vol. 487, 545.
- 5 46 P. D. Renfrew, T. W. Craven, G. L. Butterfoss, K.
6 Kirshenbaum, R Bonneau, *J. Am. Chem. Soc.* 2014, **136**, 8772.
- 7 47 K. Drew, et. al. *PLOS ONE*. 2013, **8**, e67051.
- 8 48 J. C. Miner and A. E. García, *J. Phys. Chem. B.* 2017, **121**,
9 3734.